

1
2
3
4
5
6
7
8
9
10
11
12
13
14
15
16
17
18
19
20
21
22
23
24
25
26

ELECTRON DIFFRACTION AND ELECTRON MICROSCOPY STUDY OF FILMS CuGaS_2 .

Abstract

In present work, the results of electron diffraction investigations of structures of amorphous thin films of CuGaS_2 have given and function of radial distribution of atoms (FRDA) have been calculated. Appropriate coordination number $n=4,1$ we obtained from calculating the area under the first peak, also indicates tetrahedral surrounded by atoms of copper and gallium. During the deposition of this ternary compound on a substrate with $T = 423-433$ K is formed by a mixture of polycrystalline single crystal. With the increase of temperature the intensity of polycrystallines decreases and point reflections according to the monocrystal increases. Further increase of the substrate temperature to 453 K LiF leads to the formation of a perfect single crystal.

Superstructure phase CuGaS_2 is oriented (100) plane parallel to the faces LiF. During epitaxial growth on LiF CuGaS_2 one unit cell superstructure is mated with four cells of the substrate. Between periods of lattices of the initial phase and superstructure there are simple relations common with: $a \approx 3a_0$; $c \approx 2c_0$.

Keywords. Diffraction, phase, atoms, structure, superstructure, amorphous, compositions

27 **1.Introduction.**

28 A number of works [1-3] were devoted to X- ray studies of crystalline structures
29 of the compounds of group A¹-B³-C⁶. However in none of the known works
30 patterns of short range order structure of amorphous compositions CuGaS₂ were
31 determined.

32 The reason for this can be found either by difficulties in establishing
33 conditions for amorphous films of these compounds, or trends in amorphous films to the
34 more dense packing.

35 Amorphous thin films CuGaS₂,
36 of thickness 25 nm were obtained by evaporation alloys CuGaS₂ in the vacuum of 10⁻⁴
37 PA on the substrate *NaCl, KCl*
38 and LiF located at room temperature. The rate of deposition of films for all cases was the
39 1.5 nm /sec. Amorphous phase CuGaS₂ is formed until T_s=383 K, crystallization,
40 which can lead to the formation of polycrystalline with periods of a tetragonal lattice,
41 military data [5].

42 Amorphous films formed with values $S=4\pi\sin\theta/\lambda=24.10; 29.50; 53.70; 83.70 \text{ nm}^{-1}$
43 (Fig.1) after heat treatment at T_s=380 K are crystallized in the structure of chalcopyrite
44 tetragonal lattice CuGaS₂ with periods a=0,535; c=1.047 nm, $CBC I\bar{4} 2d$ [5].

45 **2. Experiment**

46 Parameters of
47 short range order distances of coordination spheres and interatomic distances, coordinatio
48 n numbers (CN) may be determined by the functions of atom radial distribution (FARD) pr
49 epared according to

$$50 \quad 4\pi r^2 \rho(r) = 4\pi r^2 \rho_0 + \frac{2r}{\pi} \int_0^{\infty} Si(S) \sin(sr) dS \quad (1)[4],$$

51 the retraining Fourier intensity of the coherent scattering of electrons. Reliable, (FARD) c
 52 an only be obtained when integrating from 0 to ∞ or before S_2 , if interference
 53 functions do not feel out of oscillate that occurs in strongly disordered systems.
 54 The intensity of scattering can be determined experimentally with sufficient accuracy
 55 only on some interval of values $S=4\pi\sin\theta/\lambda$, so practically the integration in (1)
 56 is over a finite interval from S_1 to S_2 .

57

58 **3. Results and discussion**

59 Intensity curve electron scattering from amorphous films CuGaS_2 were obtained by us
 60 on electronography brand EMR-102 in the form of graphs of dependences
 61 of the intensity of scattering angles, i.e. from $S=4\pi\sin\theta/\lambda$ (Fig.1).

62 Function $i(S)$

63 graphically depicted in (Figure 2.), were used to calculate (FARD) for CuGaS_2 (fig. 3.) acc
 64 ording to formula (1). The calculation was carried out on the programmer "RADIADIS" on
 65 the computer IBM. Intervals of variables accounted for $\Delta r = 0,01 \text{ nm}^{-1}$, $\Delta S = 0,01 \text{ nm}^{-1}$.
 66

67 (FARD) CuGaS_2 (fig. 3.) contains four asymmetric highs one of which is isolated and a
 68 group of false highs, emanating from the larger values of S .

69 The area under the respective highs, manifesting themselves in $r_1 = 0,234$; $r_2 = 0,244$;
 70 $r_3 = 0,282$; $r_4 = 0,411 \text{ nm}$. are equal $\Delta_1 = 16,0$; $\Delta_2 = 20,3$; $\Delta_3 = 55,5$ and $\Delta_4 = 80,0$
 71 nm respectively.

72 Distance $r_1 = 0,234$ nm revealed on (FARD) CuGaS_2 , is the distance between
73 atoms Cu-S, as tetrahedral covalent radii are equal to $r_{\text{Cu}} = 0,135$ and $r_{\text{S}} = 0,104$
74 nm. Appropriate coordination number $n=4,1$ we obtained from calculating the area
75 under the first peak, also indicates tetrahedral surrounded by atoms of copper
76 and gallium.

77 Radius of the second coordination sphere equal to $r_2 = 0,244$ nm which we were
78 able to interpret as the distance Ga-S. The ionic radii of gallium and sulfur atoms
79 constitute $r_{\text{Ga}} = 0,127$ and $r_{\text{S}} = 0,104$ nm, for which coordination number is six.
80 Meaning coordination number equal to $n_2 = 6,3$ received by us from calculating
81 the area of the second peak on (FARD) CuGaS_2 also indicates the octahedral environment
82 of gallium atoms by sulfur atoms.

83 The bond length between the atoms equal to $r_3 = 0,282$ nm corresponds to the
84 distance between the same atoms Ga-Ga. Fourth maximum detected at a distance
85 nm can be referred to the distance between the negatively charged divalent atoms (S^{2-}).
86 It should be noted that on (FARD) CuGaS_2 arise false details too, and they
87 may arise due to errors in the experimental intensity curve or cliff: they are mainly manifes
88 ted in the large values of S and belong to groups with slightly blurred large
89 coordination number equal to 8, 10 and 12.

90 During the deposition of this ternary compound on the substrate with $T_s = 423$ -
91 433 K a mixture of polycrystalline with single crystal is formed (Fig. 4.).

92 On the electron from the mixture appears more additional weaker reflexes appear. As a
93 result of increase of temperature intensity polycrystalline lines are reduced but the
94 intensity of point reflections corresponding to single crystal grow.

95 Further increase of the substrate temperature to 453 K LiF leads to the formation of
96 a perfect single crystal. On electron diffraction from single crystals
97 (Fig. 5), discontinued at right angles strong point reflexes, forming a square grid
98 displayed on the basis of $hk0$ reflexes known lattice CuGaS₂. Indexing of all
99 reflexes, including additional low in intensity lines is achieved with parameter
100 $a = 1.605$ nm.

101 Period "c", established by electron diffraction, shot at an angle $\varphi = 35^\circ$ was found to be
102 2.102 nm.

103 Between periods of lattices of the initial phase and superstructure there
104 are simple relations common with: $a \approx 3a_0$; $c \approx 2c_0$. In the electron derived from film
105 on substrates formulated with higher temperatures ($T_s = 473$ K), dynamic effects
106 appear (Figure 6.). The microstructure of single
107 crystal layers CuGaS₂ from which there is a dynamic high energy electron scattering is shown
108 in Fig. 7 (X 20000). Thus, substrates can be LiF CuGaS₂ samples with varying substructure
109 including a super lattice phase super period. Growth mechanism of single-crystal
110 thin - film and nano scale epitaxial films is a model for many heterogeneous and
111 topochemical processes.

112 However, the existing theory of crystallization cannot explain all of the results of a large amount
113 of experimental work -

114 there is a clear discrepancy between the flow: The totality of new facts and their level of theoretical
115 understanding of the experimentally observed facts with a unified position cannot
116 be considered. In existing theories of crystallization there is still no consensus on
117 what is the main factor in orienting epitaxial.

118 Generally accepted explanation is not considered as such a statement and that the main fact
119 or in orienting epitaxial is a single-crystal structure -
120 substrates. Focused on the growth of amorphous boundary layers prepared on the surface o
121 f the substrate crystals [6,7], is proof that the basic structure of crystals does not
122 determine substrate orientation effects .
123 Oriented crystallization on the outside boundary of polycrystalline layers [8-
124 9], as well as the growth of not only epitaxial films, but also highly perfect single
125 crystals through the amorphous boundary
126 layers [10] makes relate to the theory of crystallization based on the structure of single-
127 crystal substrates seeds very carefully. Since many experimental
128 works performed revealed a clear discrepancy between the facts and their level of theoretic
129 al understanding, it is not yet possible to formulate some general criteria for the formation o
130 f epitaxial films and single crystal. Therefore, conditions for the formation of single-
131 crystal films to day, as shown in the previous chapter, are
132 established only experimentally.
133 Since the bulk crystal lattice CuGaS_2 ordered, in order to explain the
134 formation of super lattice phase should assume that it is the disordered phase. Disorderin
135 g ordered - structures some of the initial
136 of the atoms in it are defective, resulting superstructure should have a statistical average fr
137 equency. Regularities of similar phase transitions were first established for the phases of
138 the chemical group of compounds $\text{A}^3\text{B}^3\text{C}^6$ [4].
139 Superstructure phase CuGaS_2 is
140 oriented (100) plane parallel to the faces [11] LiF. During epitaxial growth on LiF CuGaS_2
141 one unit cell (UC) superstructure is

142 mated with four cells of the substrate. Relative discrepancy mating crystal lattices in this
143 case is 2,9%.

144

145 **Literature**

146 1. Bodnar I.V., Rud V.Y., Rud J.V., Breeding and research properties of ternary compounds
147 CuGa₃Se₅ // Neogame. 2002, I. 38, № 9, s-875.

148 2. Bodnar I.V., Rud and V.Y..Rud Y.V. Novel I-III-VI₂ semiconductor-native protein structures
149 and their photosensitivities // Semicond. Science and Technology. 2002,v. 17, N 10,p. 1044-
150 1047.

151 3. Orlova N.S., Bodnar I.V., Kushner T.L., Kudritskaya E.A. Crystal Growth and properties of
152 the Compounds CuGa₃Se₅ and CuIn₃Se₅ // Cryst. Res. Techn. 2002. v. 3, N 6, p. 540-550.

153 4. Ismailov DI phase formation, structure and kinetics crystallization in thin films A₃-B₃-s ,
154 epitaxial growth superstructural phases. Dis.... math.menboku, 2007,345 S.

155 5. Foseco-chemical properties of semiconductor materials : / Handbook Ed. Novoselova AVI
156 Lazareva V.B. have been Nauka, 1979,s.

157 6. B.K. Vainshtein Structural electronography. M: Izd. An SSSR, 1956, 315 S.

158 7. Gerasimov, Y.M. of Distler GI Orientirovannayakristallizatsiya gold on the surface of the
159 crystal NaU through amorphous carbon film // Kristallografiya, 1969, I. 14, number 6, C. 1101-
160 1104.

161 8. The distler GI Tokmakova E.I. Issledovanie epitaxial Rasta sulfur lead through boundary
162 amorfnykh copying the electrical structure of the surface of crystals // crystallography, 1971, T.
163 16, no 1, S. 212-217.

164 9. The distler GI of ObrosoV V.G. Photoelectron mechanism dalnodeystvie transmission and
165 storage of structural information polikristallicheskom and single crystal boundary layers // Dokl.
166 An SSSR, 1971, so 197, № 4, S. 819-832.

167 10. Discharge Lobachev A.N. V.P. Vlasov other new method of breeding single crystals // Dokl.
168 An SSSR, 1974, so 215, № 1, S. 91-94.

169 11. Bodnar I.V., Bodnar IT, Viktorov I.A., O. Obratzsova. Cultivation, structure and optical
170 properties of single crystals triple connection CuGa5Se8// ZhPS, 2005, so 62, no. 1, S. 544-548.

171

172

173

174

175

176

177

178

179

180

181

182

183

184

185

186

187

Figures of ELECTRON DIFFRACTION AND ELECTRON MICROSCOPY STUDY OF FILMS CuGaS₂.

188

189

190

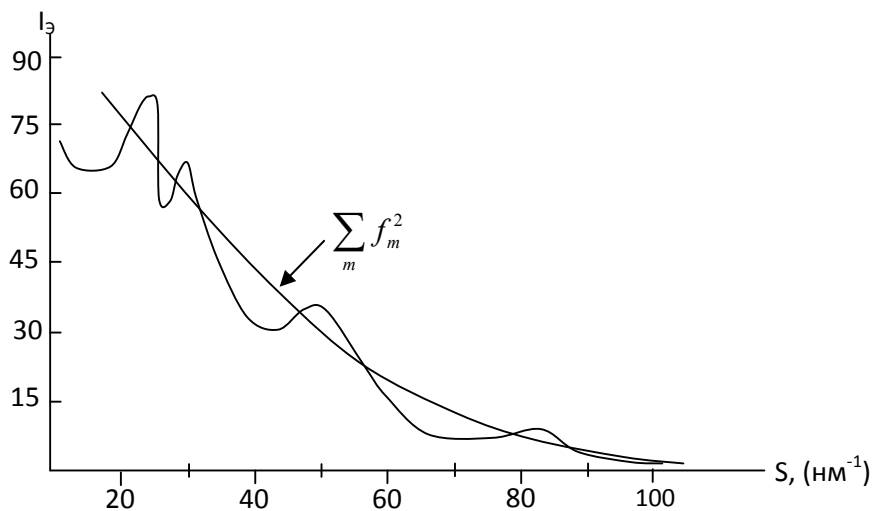
191

192

193

194

195



196

Fig.1.

197

198

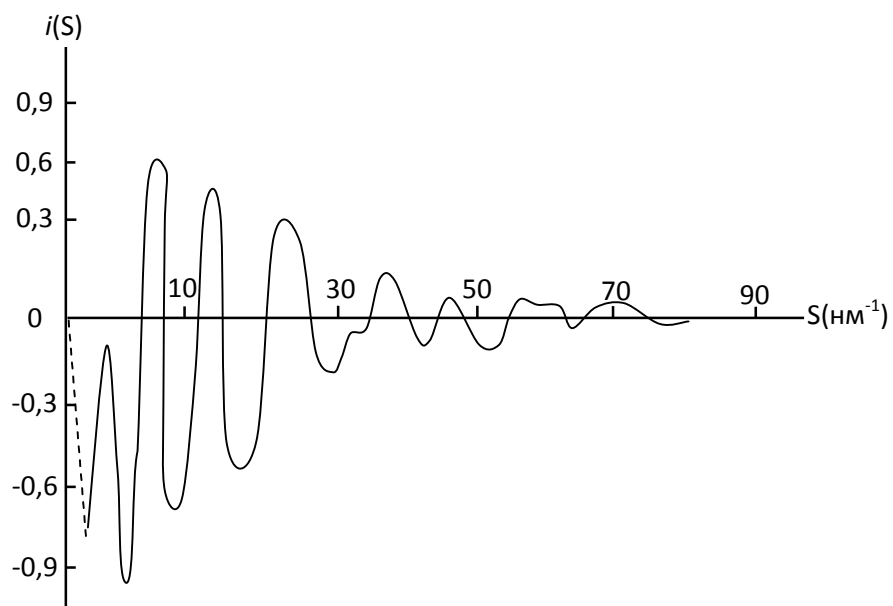
199

200

201

202

203



204

205

206

207

208 Fig.2.

209

210

211

212

213

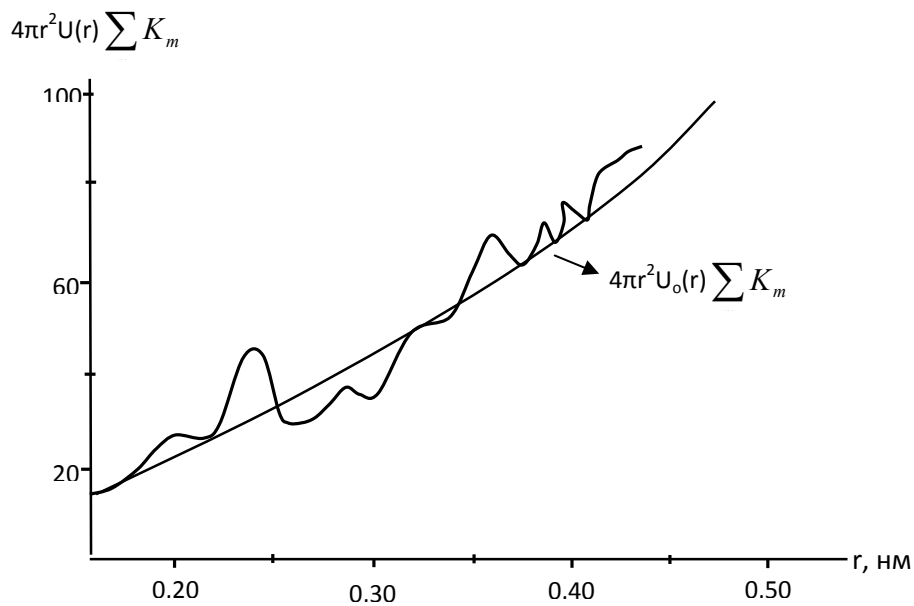
214

215

216

217

218



219

220

221

222

223

224

225

226

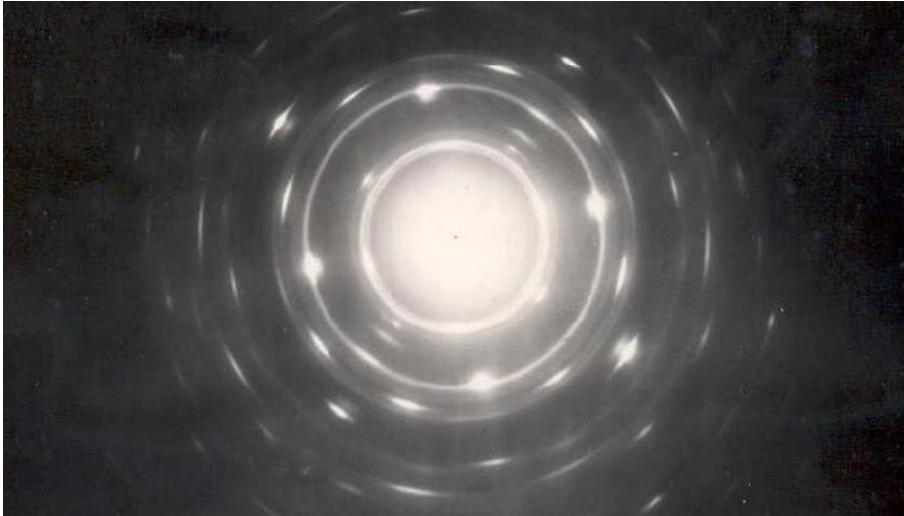
227

228

229 Figure 3.

230

231

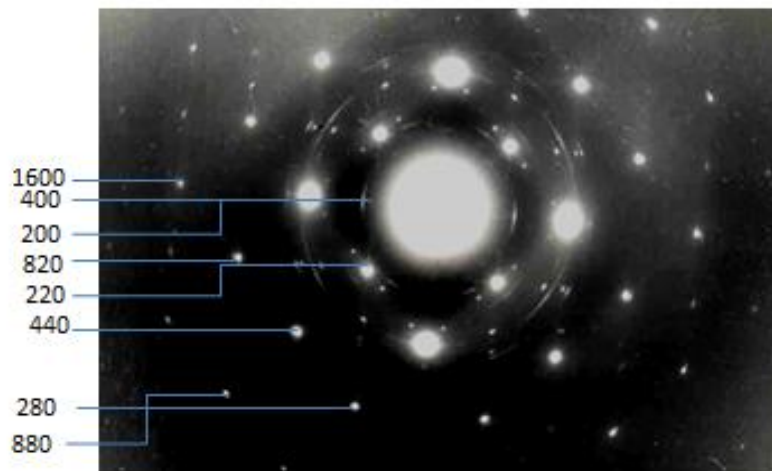


232

233

234 Fig. 4.

235



236

237

238

Fig.5.

239

240

241

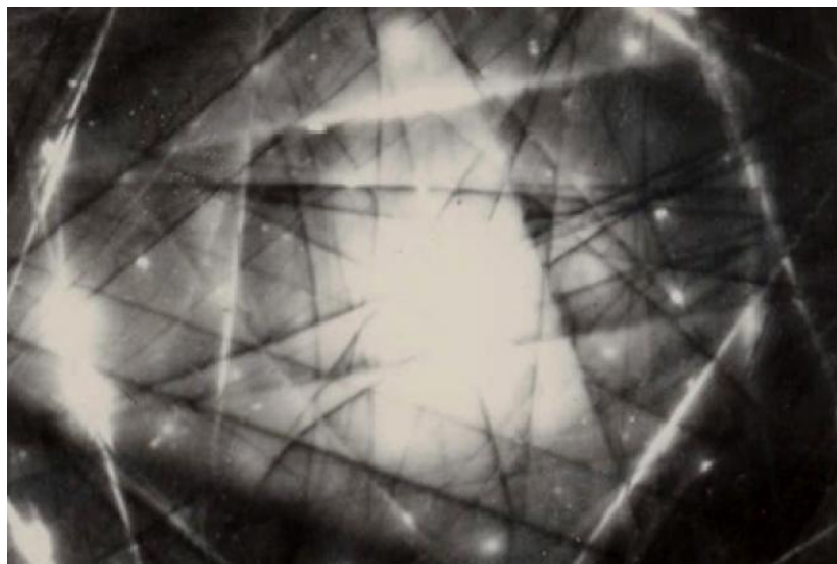
242

243

244

245

246

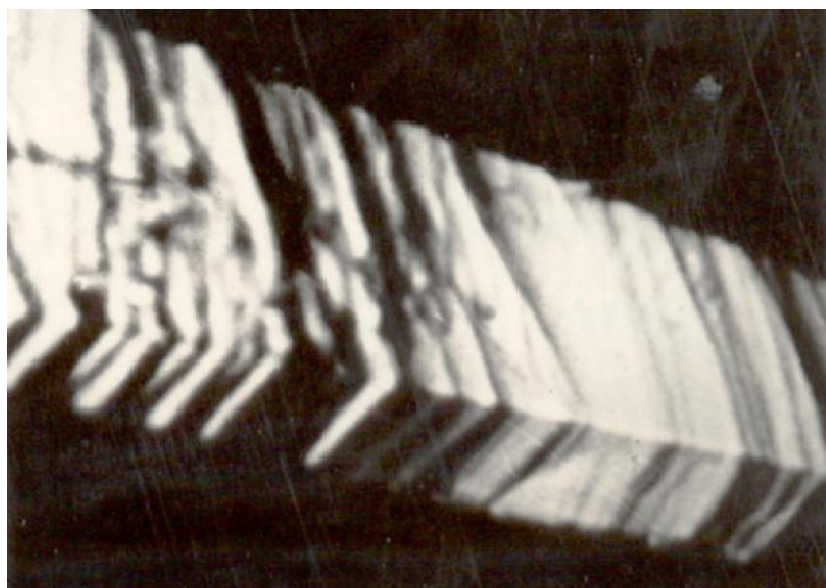


247

248

249 Fig.6.

250



251

252

Fig. 7.

253
254
255
256
257

Captions to figures of **ELECTRON DIFFRACTION AND ELECTRON
MICROSCOPY STUDY OF FILMS CuGaS₂**.

258 Fig.1. The intensity curves of amorphous CuGaS₂.
259
260 Fig.2. Interference scattering function of electrons of amorphous CuGaS₂
261
262 Fig.3. The curve of radial distribution of atoms of CuGaS₂
263
264 Fig. 4. Electron diffraction single crystal mixture with polycrystalline CuGaS₂
265
266 Fig.5. Electron diffraction from single crystal super lattice phase CuGaS₂
267
268 Fig.6. Electron diffraction pattern with Kikuchi lines from
269
270 single crystal CuGaS₂ high perfections.
271
272 Fig. 7. The microstructure of single-crystal beds of CuGaS₂ (H20000).
273